Archimer
http://archimer.ifremer.fr

Hydrothermal faunal assemblages and habitat characterisation at the Eiffel Tower edifice (Lucky Strike, Mid-Atlantic Ridge)

Daphne Cuvelier[1, *], Pierre-Marie Sarradin[2], Jozée Sarrazin[2], Ana Colaço[1], Jon T. Copley[3], Daniel Desbruyères[2], Adrian G. Glover[4], Ricardo Serrão Santos[1], Paul A. Tyler[3]

[1] IMAR & Department of Oceanography and Fisheries, University of the Azores, Horta, Portugal
[2] Institut Français de Recherche pour l'Exploitation de la Mer (Ifremer), Centre de Brest, Département Études des Écosystèmes Profonds, Laboratoire Environnement Profond, Plouzané, France
[3] School of Ocean & Earth Science, University of Southampton, Southampton, UK
[4] Zoology Department, The Natural History Museum, London, UK

*: Corresponding author : Daphne Cuvelier, email address : daphne.cuvelier@gmail.com

Abstract :

The Eiffel Tower edifice is situated in the Lucky Strike hydrothermal vent field at a mean depth of 1690 m on the Mid-Atlantic Ridge (MAR). At this 11-m-high hydrothermal structure, different faunal assemblages, varying in visibly dominant species (mussels and shrimp), in mussel size and in density of mussel coverage, were sampled biologically and chemically. Temperature and sulphide ($\sum S$) were measured on the different types of mussel-based assemblages and on a shrimp-dominated assemblage. Temperature was used as a proxy for calculating total concentrations of CH_4. Based on the physico-chemical measurements, two microhabitats were identified, corresponding to (i) a more variable habitat featuring the greatest fluctuations in environmental variables and (ii) a second, more stable, habitat. The highest temperature variability and the highest maximum recorded temperatures were found in the assemblages visibly inhabited by alvinocaridid shrimp and dense mussel beds of large *Bathymodiolus azoricus*, whereas the less variable habitats were inhabited by smaller-sized mussels with increasing bare surface in between. Larger mussels appeared to consume more $\sum S$ compared with smaller-sized (<1 cm) individuals and thus had a greater influence on the local chemistry. In addition, the mussel size was shown to be significantly positively correlated to temperature and negatively to the richness of the associated macrofauna. The presence of microbial mats was not linked to specific environmental conditions, but had a negative effect on the presence and abundance of macro-fauna, notably gastropods. Whereas some taxa or species are found in only one of the two microhabitats, others, such as polychaetes and *Mirocaris* shrimp, cross the different microhabitats. Temperature was proposed to be a more limiting factor in species distribution than $\sum S$.

Keywords : Faunal assemblage ; hydrothermal vent ; microhabitat ; Mid-Atlantic Ridge ; physico-chemical characterisation

1. Introduction

Hydrothermal ecosystems are extremely variable environments, characterised by elevated temperatures relative to ambient deep-sea water. However, with only a few exceptions, the temperatures most vent species live at are no different from those in shallow-water habitats and it is the chemistry and composition of the fluids that sustain life at hydrothermal vents (Jannasch 1985). Steep thermal and chemical gradients exist and turbulent mixing occurs between the hydrothermal fluids and cold surrounding seawater, resulting in high local variability, on a scale of a few centimetres (Johnson *et al.* 1988a; Chevaldonné *et al.* 1991; Sarrazin *et al.* 1999, 2006; Le Bris *et al.* 2006). The region wherein sulphide and oxygen co-exist, both indispensable for chemosynthesis by thiotrophic endosymbionts, is thus restricted to the interface between reduced chemicals from the hydrothermal fluids and oxygenated seawater (Johnson *et al.* 1988b; Sarradin *et al.* 2009). Attempts to define the microhabitats where species live and characterise the local faunal composition have taken place at hydrothermal vents on various Mid-Ocean Ridges and spreading centres: the East Pacific Rise (EPR: Fisher *et al.* 1988; Johnson *et al.* 1988b, 1994; Sarradin *et al.* 1998; Bates *et al.* 2005; Dreyer *et al.* 2005; Govenar *et al.* 2005; Sarrazin *et al.* 2006; Mills *et al.* 2007; Lutz *et al.* 2008; Matabos *et al.* 2008); the Juan de Fuca Ridge (JdF: Sarrazin & Juniper 1999; Sarrazin *et al.* 1999; Tsurumi & Tunnicliffe 2003; Urcuyo *et al.* 2003); Lau Basin (Henry *et al.* 2008; Podowski *et al.* 2009); and the Mid-Atlantic Ridge (MAR: Sarradin *et al.* 1999; Desbruyères *et al.* 2000, 2001). Evidence for the close association of vent community development with physico-chemical conditions has already been demonstrated (Luther *et al.* 2001). According to changing physico-chemical conditions, hydrothermal vent edifices may be inhabited by faunal assemblages that form repeating mosaics (Sarrazin *et al.* 1997, 1999).

68

The Eiffel Tower edifice of the Lucky Strike vent field (1690m depth) is located on the shallower part of the MAR. It is visibly dominated by *Bathymodiolus azoricus* that forms extensive mussel beds (Desbruyères et al., 2001). A variety of taxa live in association with these mussel beds, including alvinocaridid shrimps and a decapod crab along with less conspicuous fauna such as polychaetes, gastropods, amphipods and pycnogonids etc. (Desbruyères et al., 2006). At the Eiffel Tower hydrothermal edifice, Cuvelier et al. (2009) identified 4 visibly different faunal assemblages of which 2 had a sub-form. Assemblage 1 was visibly dominated by dense beds of larger-sized mussels, while Assemblage 2a featured mussel clumps with bare surface in between. Assemblage 2b was similar to Assemblage 2a but contained visible microbial mats. Assemblage 3 represented bare surfaces colonised by shrimps. Assemblage 4a resembled bare substrata with small dispersed mussels, whereas Assemblage 4b was similar to Assemblage 4a but with visible microbial mats.

81

Using image analysis, a faunal zonation model around a fluid exit has been proposed for the Eiffel Tower edifice (Cuvelier et al., 2009). Based on the distribution patterns and proximity to the fluid exits of the faunal assemblages, the existence of at least two microhabitats was hypothesised. These microhabitats were thought to correspond to a "harsher" (higher temperature, higher sulfide) environment, inhabited by shrimps and larger-sized mussels, while the other assemblages, featuring smaller-sized mussels and a less dense coverage, were thought to be characterised by lower levels of T°C and sulfide. However, since this model was primarily based on video imagery, it requires confirmation through biological sampling. Hence the primary objectives of this study are: (a) to examine macrofaunal composition in visibly different assemblages, (b) to identify the microhabitats inhabited by the different faunal assemblages, (c) to evaluate if variability in physico-chemical factors corresponds to visible faunal differences (size of mussels, presence of microbial cover and species composition/dominance) and (d) to analyse if the microhabitats identified correspond to the previously hypothesised microhabitats.

96

97

98

Material and methods

Study area

Lucky Strike is a basalt-hosted vent field (Langmuir et al., 1997; Fouquet et al., 1998, Ondréas et al., 2009) situated on the shallow part of the MAR, at a mean depth of 1700m, and was visually observed for the first time in 1993 (Fig. 1). It is characterised by a central lava lake, around which the hydrothermal vent edifices are located (Ondréas et al., 2009). The Eiffel Tower sulfide structure is situated in the south-eastern sector, on the saddle between two volcanic cones. It is an 11m high active edifice and one of the most visited sites within this vent field.

Faunal assemblage sampling

During the MoMAR08 cruise (August 2008, NO l'Atalante), semi-quantitative biological samples were taken with the Remotely Operated Vehicle (ROV) Victor 6000 on visibly different assemblages, which correspond to those identified by Cuvelier et al. 2009 (Fig. 2). Biological sampling was undertaken to investigate the macrofaunal species composition of these assemblages. To facilitate the description of the results, we will refer to the samples taken with the name of the assemblages they correspond to. Accessibility and manoeuvring space for the ROV were prime determinants in choosing a sampling location. Samples (three to four grabs) were taken with the manipulator arm of the ROV and placed in a sampling box, followed by a clearing of the sampled surface with the slurp gun/suction sampler. The faunal sampling of Assemblage 4b failed due to a hydraulic problem of the ROV, and was therefore left out of the analyses.

When the biological samples arrived on board, the macro-and megafauna received the highest attention and organisms were immediately identified to the lowest taxonomic level possible. Specimens were subsequently fixed in seawater buffered formalin (10%) and after 48 hours transferred to 70% ethanol. The surfaces sampled were measured with pixel-based image analysis software IPLAB Spectrum® as described in Sarrazin et al. (1997), in which the manipulator arm of the ROV was used as a scale (Table 1). The crab *Segonzacia mesatlantica* was not considered in the statistical analysis, because this species is highly mobile and tends to escape when approached with sampling equipment, hence it could not be considered representative. Finally, the empty gastropod shells of *Shinkailepas briandi* present in two different samples were noted in the density table but were not considered in the statistical

132   analyses, since these appeared to be remnants of a senescent population. Chemical sampling
133   was carried out in a consecutive dive.
134

Chemical sampling

136   The CHEMINI (CHEmical MINIaturised) analyser was used to measure *in situ*
137   concentrations of sulfides among the fauna (Vuillemin et al., 2009). The inlet of the analyser
138   was directly mounted on the temperature probe manipulated by the ROV Victor 6000. Hence
139   temperature and total dissolved sulfides ($\sum S = H_2S$, HS^-, S^{2-}), hereafter referred to as $\sum S$, were
140   measured during 10 minutes among the different assemblages. Chemical sampling was
141   carried out in an undisturbed region of each sampled assemblages. A reference sample was
142   taken away from the hydrothermal active area, to calibrate the sensor against bottom seawater.
143   Calibration of the analyser was done *in situ*, at the beginning and at the end of the dive.
144   Sampling time stamps were noted during the dive and afterwards measurement results were
145   refined by looking at the video imagery. Data from when the CHEMINI probe was not
146   touching the fauna (due to involuntary ROV movements caused by currents) were eliminated
147   to avoid measurements of surrounding seawater. Total concentrations of CH_4 were calculated
148   from these *in situ* values, using a T°C vs. CH_4 regression curve obtained for Eiffel Tower
149   hydrothermal fluids during the same cruise (Sarradin et al., in prep.).
150

Statistics

152   Principal Component Analysis (PCA) was carried out with the Vegan package (Oksanen et
153   al., 2008) in R (version 2.8, Multicore team 2008) based on species abundance data. The
154   species abundance-matrix was subject to a Hellinger-transformation prior to statistical
155   analyses. Hellinger transformation is calculated by taking the square root of observed values
156   divided by the row (site) totals and is very useful for community data, making them suitable
157   for linear ordinations (Legendre & Gallagher, 2001). Taxonomic richness and rarefaction
158   were also calculated with the Vegan package, while Spearman Rank Correlations among the
159   chemical factors were carried out in Statistica 6 (StatSoft Inc. 2001). Preference was given to
160   Spearman Rank Correlations as these are less sensitive to outliers and do not require
161   normality of the data. As the data matrix did not meet the assumptions for parametric testing,
162   not even after transformations, differences between the environmental variables (T°C and $\sum S$)
163   were analysed with non-parametric tests (Kruskal-Wallis followed by post-hoc Wilcoxon
164   pairwise testing), which were performed in R. Since CH_4 was estimated based on the
165   temperature values, it was not used in the statistical analyses.

Results

Faunal assemblage sample composition

The visible assemblage identification at Eiffel Tower is given in Figure 2, while an overview of the fauna present in the sampled assemblages is presented in Table 1. The density data showed that samples from Assemblages 2a and 4a were dominated by the same three species, starting with *Bathymodiolus azoricus*, the gastropods *Protolira valvatoides* and *Lepetodrilus atlanticus* and the polynoid polychaete *Branchipolynoe seepensis*. Assemblage 1 was also dominated by *B. azoricus* but the second dominant species was the shrimp *Mirocaris fortunata*, followed by *B. seepensis* and *Amathys lutzi* polychaetes. Assemblage 3 was almost exclusively dominated by *Mirocaris fortunata*, which were also very abundant in Assemblage 2b. The second dominant species for both assemblages was the amphipod *Luckia striki*, together with an undetermined polynoid polychaete in Assemblage 3. *Luckia striki* had the highest abundance in Assemblage 2b.

The mytilid individuals showed significant differences in mussel lengths (Kruskall Wallis, H=41.71, $p<0.001$, df=3). Assemblages 2a and 2b measured between 2 and 5 cm (no significant differences between them, but significantly different from Assemblages 1 and 4a $p<0.05$) while the mean size of the individuals in Assemblage 4a was about 1 cm (significantly different from Assemblages 1 and 2, $p<0.05$). The mussel length in Assemblage 1 was significantly higher ($p<0.001$), with a mean of 6 cm. The size or length distribution of the mussels was as follows: Assemblage 4a < Assemblages 2 < Assemblage 1. There were no mussels in Assemblage 3. Gastropods were only present in the assemblages with smaller to medium-sized mussels without visible microbial cover (Assemblages 2a and 4a), while polychaetes had the highest abundance in the larger-sized mussel beds (Assemblage 1). *Branchipolynoe seepensis* lives inside the mussel shells of *B. azoricus*. This commensal polychaete had the lowest abundance when the size of the mussels was smallest (i.e. in Assemblage 4a), however its abundance did not increase in proportion to the mussel shell size. The ratio of the number of *B. seepensis*/number of mussels was highest in the medium-sized mussels of Assemblage 2b followed by Assemblage 1 with the larger mussels. Assemblage 4a had a unique presence of the pycnogonid *Sericosura heteroscela*. The crab *Segonzacia mesatlantica* was present in 3 samples: 4 individuals were sampled in Assemblage 1, 2 in Assemblage 2b and 2 in Assemblage 3.

198   Taxonomic richness and rarefaction were calculated to evaluate which sample of which
199   assemblage was the most diverse (Table 1). The highest richness was found in Assemblage 4a
200   with 11 taxa present, while Assemblage 3 was the least diverse (Table 1). In these
201   calculations the undetermined species also counted as species, as they were different from the
202   determined species. When calculating the expected number of species (Es) present in a sub-
203   sample of size 100 (rarefaction or Es(100)), similar trends were apparent (Table 1). Mussel
204   sizes showed negative relationships with taxonomic richness (R^2=0.67) and Es(100)
205   (R^2=0.81).

206

207   **Physical and chemical characterisation**
208   Overall, a narrow temperature range (<2°C) was observed between the different assemblages
209   (Fig. 3). However, some variability was noticeable as the temperature tended to oscillate,
210   resulting in a broader temperature range for certain assemblages (Fig. 3). The minimum
211   temperature measured was 4.44°C in Assemblage 2b, i.e. very close to the seawater
212   temperature (4.4°C) (Table 2). The highest temperature (9.54°C) was measured in
213   Assemblage 3 (Table 2). The shrimp assemblage (Assemblage 3) thus tolerated the highest
214   temperatures recorded and the highest degree of temperature fluctuations (up to ~4.4°C),
215   while both Assemblages 4a and 4b were very stable, exhibiting the lowest degree of
216   fluctuations (Fig. 3). Of the mussel-based assemblages, Assemblage 1 with the larger-sized
217   mussels had the broadest range (~1.56°C) and the highest maximum temperature (6.14°C)
218   (Fig. 3).

219

220   Among the different environmental factors, temperature and ΣS were positively and
221   significantly correlated (r=0.42, p<0.05, df=38). As CH_4 was estimated based on the
222   temperature, it showed exactly the same trends and is therefore not considered in further
223   detail here. A non-parametric Kruskal-Wallis test confirmed significant variations in both
224   temperature (H=576.55, p<0.001, df=5) and ΣS values (H=26.16, p=0.001, df=5) on the
225   different faunal assemblages (Fig. 4).

226

227   The temperature values measured in Assemblage 1 showed the largest variations, when
228   compared to the other mussel-based assemblage values. The mussel clumps of Assemblage
229   2a had a higher mean temperature than Assemblages 1 and 2b. Assemblage 4b had a
230   significantly higher temperature than Assemblage 4a (p<0.001), a trend opposite to that
231   observed between Assemblages 2a and 2b (Fig. 4a). Post-hoc testing revealed that

232   differences in the temperature values between all the assemblages were significant (p<0.001)

233   except between Assemblages 1 and 4b (p>0.05).

234

235   For the ∑S values, the differences between the different assemblages were less pronounced

236   (Table 2, Fig. 4b), with concentrations ranging from 0.4 to 28 µM. Assemblage 3 exhibited

237   the broadest range and the highest values. Assemblages 4a and 4b exhibited higher ∑S values

238   than the other mussel assemblages, while ∑S concentrations were lower in Assemblages 1,

239   2a and 2b (Fig. 4b). Contrary to their temperature values, the ∑S-values of Assemblages 4a

240   and 4b were closer to those of Assemblage 3 than the other assemblages. The differences

241   between Assemblages 1 and 2 were not significant for ∑S (p>0.1). Significant differences are

242   found between Assemblage 2b and Assemblage 3 (p<0.05), between Assemblage 4a and

243   Assemblages 1, as well as between Assemblages 4a and 2b (p<0.05).

244

245   **Habitat characteristics**

246   When plotting the temperature vs. the concentrations of ∑S measured within the different

247   faunal assemblages, all the points are limited to quite a narrow range (Fig. 5) with a strong

248   curvature in the smoothed dilution curve. Assemblage 3 clearly had the broadest temperature

249   range and the highest concentrations of ∑S. The microhabitats of the larger- and medium-

250   sized mussels (Assemblages 1 and 2) were consistent. The T°C-∑S values measured in the

251   larger-sized mussel beds of Assemblage 1 were positioned on a gentle slope (slope of

252   curve=1.92). The mussel clumps with microbial mats (Assemblage 2b) had slightly lower ∑S-

253   values than the mussel clumps without microbial cover (Assemblage 2a), which also had a

254   higher temperature than the former (Table 2, respective slopes are 1.67 and 3.02). The

255   plotting of Assemblages 4a and 4b above the observed dilution curve (Fig. 5), highlights their

256   elevated levels of ∑S compared with the temperature and the ratios of the other mussel-based

257   assemblages (Table 2). Both had steep slopes in the T°C-∑S curve, for which the slope of

258   their curves are 7.19 for Assemblage 4a and -13.19 for Assemblage 4b. Even so, the

259   assemblage with microbial cover (4b) had lower ∑S-values for higher temperatures than the

260   same assemblage without visible microbial mats (Assemblage 4a).

261

262   **Fauna-habitat relations**

263   Ordinations with Hellinger-transformed species abundance data were used to unravel patterns

264   between species and assemblages (Principal Component Analysis (PCA), Fig. 6). A total

variation of 92.4% was explained by the first two axes, of which the first axis accounted for
79.6% (Fig. 6). Assemblages for which the distance separating them equals zero are
considered similar. Therefore Assemblages 2a and 4a as well as Assemblages 1 and 2b were
considered more similar regarding their species composition and abundance, while
Assemblage 3 was more distinct from the others. The positioning of Assemblages 1, 2b and 3
was largely influenced by the abundance of *Mirocaris fortunata* in these assemblages.
Assemblages 2a and 4a were considered similar because of the shared abundance of
Lepetodrilus atlanticus and *Protolira valvatoides* gastropods. In addition to *Bathymodiolus*
azoricus, the mussel-based assemblages (i.e. Assemblages 1, 2a, 2b and 4a) are characterised
by the presence of different polychaete taxa.

When plotting histograms of the percentage of temperature measurements in categories
separated by 0.5°C, preference for a certain temperature regime was revealed for each
assemblage (Fig. 7). All mussel-based assemblages grouped together in the colder
temperature array (4.44°C-6.14°C), while the shrimp assemblage had the broadest range in
the warmer temperatures (5.18°C-9.54°C). Two temperature niches were thus revealed. In
addition, a significant positive correlation was observed between the mussel size and the
temperature, where the increasing mussel size corresponded to increasing temperature
(R^2=0.9986, p<0.01, df=27, Fig. 7). The larger-sized mussels of Assemblage 1 had the
broadest range and the highest temperature, overlapping in temperature with the beginning of
the shrimp-niche. Assemblage 2a is present in the 5-6°C range, while Assemblage 2b spanned
4-5°C, with a higher numbers of measurements between 4.5-5°C. Assemblage 4a had 100%
of its measurements in the range 4.5°C-5°C, while Assemblage 4b featured higher
temperatures.

Discussion

Physico-chemical characteristics of assemblages

Widest temperature and $\sum$S ranges are found in the shrimp assemblage (Assemblage 3). The
second largest temperature variations are encountered in the larger-sized mussel-beds of
Assemblage 1. In the remaining assemblages, composed of medium and smaller-sized
mytilids, a narrower range of temperature values is observed. The $\sum$S measurements show
different results, as wider ranges are encountered in the assemblages featuring small dispersed

297   mussels on predominating bare surface (Assemblages 4). In other words, the $\sum$S

298   concentration of Assemblage 4a, and to a lesser extent Assemblage 4b, is higher than for

299   other mussel-based assemblages with similar or higher temperatures, e.g. Assemblages 1 and

300   2b. This might result from the preponderance of bare surface and consequently a lower

301   biological uptake by the small and dispersed animals. In fact, what we measure in the vicinity

302   of the fauna results from what is supplied by the fluids and what disappears through

303   precipitation and organism consumption.

304

305   Assemblage 3 inhabits localities with relatively high temperatures and associated high levels

306   of $\sum$S, which should be a common feature since these abiotic factors are positively correlated.

307   Within vent mussel beds, however, temperature and chemistry do not necessarily conform to

308   a conservative mixing model (Le Bris et al., 2006). The concave curvature we observe in the

309   T°C-$\sum$S plot is indicative for sulfide removal (Johnson et al., 1988b). This suggests that

310   mussels may influence chemistry by removing H_2S through their endosymbionts (Fisher,

311   1990), altering the already existing gradients (Johnson et al., 1988b). The presence of the

312   animals might also result in a higher degree of precipitation of chemicals (Sarradin et al.,

313   1999). When plotting temperature vs. $\sum$S, the medium to larger-sized mussel beds

314   (Assemblages 1, 2a and 2b) tend to group together. The $\sum$S-values in Assemblage 1,

315   associated with a broad T-range, are positioned on a gentle slope, which can imply that larger

316   mussels consume more H_2S. Assemblage 2b has a gentler T-$\sum$S slope than Assemblage 2a

317   suggesting that mussel-assemblages with, in addition to their endosymbionts, a microbial

318   cover on their shells also have a higher H_2S consumption (Le Bris et al., 2006). Assemblages

319   with the predominance of bare surface (Assemblages 4a and 4b) tend to cluster above the

320   dilution curve, approaching a proximal-plume model at Eiffel Tower (Sarradin et al., in prep.,

321   Fig. 5). Nonetheless, the measurements of the majority of mussel-based assemblages are

322   coherent with the mussel microhabitat measurements from 2006 (De Busserolles et al., 2009;

323   Vuillemin et al., 2009), except for Assemblage 4a.

324

325   At Eiffel Tower, shrimps (Assemblage 3) live closest to the fluid exits, followed by larger

326   sized-mussels (Assemblage 1) and with further increasing distance, by the smaller-sized

327   mussels in the mussel-clumps of Assemblage 2 (Comtet & Desbruyères, 1998; Sarradin et al.,

328   1999; Cuvelier et al., 2009). The distance to the fluid exits increases even more for the small

329   mussels from Assemblages 4a and 4b (Cuvelier et al., 2009). The gradient of decreasing

mussel size with increasing distance from the fluid exit observed at Eiffel Tower was suspected to correspond to a decline in temperature (Comtet & Desbruyères, 1998; Sarradin et al., 1999; Desbruyères et al., 2001), which was confirmed here, as a significant positive correlation is observed between mussel size and temperature. Overall, we discern two temperature niches, distinguishing the mussel-based assemblages from the shrimp assemblage. Despite the overlap in temperature niche and range of the larger-sized mussels of Assemblage 1 and the shrimps, mussels generally thrive in the colder regions as opposed to the shrimps that prefer warmer localities.

Environmental fluctuations provide opportunities for niche partitioning. As the different mussel-assemblages appear to occupy the same temperature niche, the individual assemblages do show differences in overlap among each other. Assemblages with microbial cover and the ones without are significantly different from each other regarding their temperature values (see Assemblages 2a-2b and 4a-4b). We could hypothesise that the microbial cover has an effect on the local environment or on the mussels either by increasing sulfide consumption or by supplying energy from chemosynthesis to the mussels. However, until now, no physiological (no significant differences in lipids, carbohydrates or total proteins) nor toxicological (no significant differences in metals and metallothioneins) differences were found between mussels with or without microbial cover (Martins et al., 2009). Additionally, the differences observed are not consistent between the sub-forms of assemblages, as Assemblage 2a has higher temperature values than Assemblage 2b while it is the other way around for Assemblages 4a and 4b. Overall, Assemblage 2a has a relative high mean temperature compared with the other mussel-based assemblages, as do Assemblages 4a and 4b, although their maximum temperature is lower than that of Assemblages 1 and 3. There are two possible explanations for this feature; the first is the ability of the mussels to divert the flow horizontally, which allows them to expand the spatially limited, redox-transition zone (Johnson et al., 1988a; 1994). As a consequence, higher temperatures tend to occur at the edges of the mussel clumps (Johnson et al., 1988b). The second explanation is that during sampling the temperature sensor touched the (underlying) rocky, thereby measuring conductive heatflow from subsurface circulation of hot hydrothermal fluids.

Previous studies have hypothesised the existence of different physico-chemical microhabitats at the Eiffel Tower edifice (Sarradin et al., 1999; Cuvelier et al., 2009), supposedly dividing it in a "harsh" (higher temperature, higher sulfide) and a "less harsh" (lower temperature, lower

364   sulfide) environment, with the shrimps and larger-sized mussels inhabiting the harshest one,

365   and the smaller-sized mussels occupying the other one. Based on the data acquired for this

366   study, these two microhabitats are characterised by variability rather than harshness, although

367   they also feature the highest and lower maximum temperatures. All values of temperature, $\sum S$

368   and CH_4 presented in this study are in concordance with previously published values for this

369   edifice and MAR mussel beds (Sarradin et al., 1999; 2009).

370

371   **Faunal characteristics**

372   *Mirocaris fortunata,* the most abundant shrimp at Eiffel Tower, can tolerate warm fluids at the

373   MAR vents (36°C; Shillito et al., 2006), which explains their presence in the warmer regions.

374   This shrimp species is an opportunist and feeds on a great variety of food items, such as

375   microbial mats and tissues of other invertebrates (Gebruk et al., 2000; Colaço et al., 2002).

376   They can be found in several mussel-based assemblages, mostly where there is a microbial

377   cover present as well as on bare substrata, with no mussels. In addition, the less gregarious

378   *Chorocaris chacei* and the more solitary *Alvinocaris markensis* also occur at Lucky Strike and

379   Eiffel Tower (Desbruyères et al., 2006). Of the latter two species, there were no individuals

380   present in our samples, even though video imagery of Assemblage 3 showed that *M. fortunata*

381   co-occur with low abundances of *C. chacei* (Cuvelier et al., 2009). The absence of certain

382   'expected' species can be explained by the 'patchy' nature of the hydrothermal vent edifices

383   along with our limited number of samples (n=5).

384

385   *Bathymodiolus azoricus* is the dominant species of the Eiffel Tower edifice and for the entire

386   Lucky Strike vent field, representing a climax-community. *Bathymodiolus* can be regarded as

387   an engineering species, offering secondary surfaces and interstitial microhabitats for other

388   organisms to occupy (Van Dover & Trask, 2000). Structurally complex localities may allow

389   the coexistence of many more species through competition-induced habitat specialization or

390   through moderation of predation (Menge & Sutherland, 1976). In this way, mytilids promote

391   biodiversity by enhancing habitat complexity and altering the local physico-chemical habitat.

392   Gastropods (mainly *Protolira valvatoides*, *Lepetodrilus atlanticus* and *Pseudorimula*

393   *midatlantica*) and even new mytilid recruits of Bathymodiolinae can be found on top of the

394   mussel shells, although gastropod presence is limited to the smaller-sized mussel-based

395   assemblages without microbial cover (2a and 4a). The microbial presence appears to exclude

396   gastropod fauna. These gastropods probably feed on the detrital layer and biofilms covering

397   these mussel shells without microbial cover, while filamentous bacteria might cause

398 difficulties for attachment and movement of the gastropods. Larger-sized mussels could filter

399 a larger amount of gastropod larvae out of the water column, inhibiting settlement. Presence

400 and abundance of polychaetes differed from that of the gastropods. The gastropods are

401 exclusively present in the smaller-sized mussel assemblages without microbial cover. While

402 several polychaete species are clearly associated with the mussels, such as *Amathys lutzi* and

403 *Branchinotogluma mesatlantica,* which live in the interstitial spaces between the mussels and

404 are present in all mussel-based assemblages. At Eiffel Tower, polynoid polychaetes are often

405 visible on the mussel beds and microbial mats. One of them, the commensal polychaete

406 *Branchipolynoe seepensis* lives in the mantle cavity of the mussels. The abundance of

407 *Branchipolynoe* is lowest in the very small mussel-based assemblages (Assemblages 4a and

408 4b), which is also visible in the PCA-plot.

409

Sample/assemblage similarity

411 The highest similarity in faunal abundances and species composition is observed between

412 Assemblages 2a and 4a, which could be a different stage of the same assemblage. It is

413 Assemblage 3 that stands out, while Assemblages 1 and 2b are more similar to one another as

414 well. Due to this high faunal similarity between the latter two, there is no clear boundary

415 between the assemblages able to withstand the highest environmental fluctuations (1 and 3)

416 and those tolerating smaller environmental variable ranges (2a, 2b and 4a). This feature of

417 species crossing the borders delineated by the variability in microhabitats is due to the

418 existence of two temperature niches wherein the mussel-based assemblages group together

419 under a colder temperature regime (4.44°C-6.14°C).

420

Richness and expected number of species

422 The least diverse assemblage is the shrimp assemblage (Assemblage 3) and is also found

423 closest to the fluid exits (Cuvelier et al., 2009). This corresponds to the most variable

424 environment and could be considered the most stressful. At first sight there seems to be an

425 increase in taxonomic richness with distance from a fluid exit with Assemblage 4a, situated the

426 furthest away from a fluid exit, showed the highest richness. The expected number of species

427 corroborated this, although differences were less pronounced. This increasing distance is

428 hypothesised to correspond to a decrease in variability/stress as well. This is confirmed as there

429 is a significant negative relation between Es(100) and the standard deviations of the

430 temperature, which are a measure for the variability. Richness is likely to be subject to the

431 surface area sampled, while rarefaction tends to mitigate this artefact. However, caution should

432 be taken as our observations are based on a small number of samples and that the evaluation of
433 species richness is largely dependant on this number of samples and the surface area sampled
434 (Gauthier et al., 2010).
435

436 **Summary**

437 At Eiffel Tower, variability rather than differences in mean conditions distinguishes two
438 microhabitats, in which temperature is proposed as being a more limiting factor than ΣS. The
439 first and most variable microhabitat (broadest ranges in temperature values), also features the
440 highest maximum temperatures, is inhabited by the alvinocaridid shrimps (Assemblage 3) and
441 the larger-sized mussels (Assemblage 1). The second, more stable habitat, is inhabited by the
442 smaller-sized mussels in clumps (without and with microbial cover respectively Assemblages
443 2a and 2b) and dispersed small mussels (without and with microbial cover respectively
444 Assemblages 4a and 4b).
445 Hydrothermal vent animals such as mussels modify the local environment as we measure and
446 perceive it. Larger mussels (present in Assemblages 1 and 2) appear to consume more ΣS than
447 smaller-sized individuals (~1 cm, Assemblage 4). A higher ΣS consumption can also be
448 postulated for the mussel clumps that have an additional microbial cover on their shells
449 (Assemblage 2a). The mussel size was also shown to be positively correlated to the
450 temperature and negatively with the associated macrofauna richness. There is no evidence of
451 the microbial cover being associated to specific environmental conditions or of its influence on
452 the local chemistry, though its presence excluded gastropod fauna. The distinction between the
453 two microhabitats is less clear when looking at species abundances. Despite several marked
454 differences in presence and abundance of species between the visibly different faunal
455 assemblages, there are species (e.g. *Mirocaris fortunata* and several polychaete species) that
456 cross the boundaries delineated by the microhabitats. This was explained by the existence of
457 two temperature niches: one for the mussel-based assemblages in the colder temperature areas
458 and the other for the shrimps in the warmer regions, with an overlap in temperature-niche
459 between the larger-sized mussels and the shrimps. A more thorough sampling at Eiffel Tower,
460 both biologically (including replicates, meiofauna assessment and different sampling
461 efficiency) as chemically (consideration of other electron donors, time-series measurements) is
462 needed to validate our findings or highlight possible other factors at play, which we were
463 unable to assess at this point. Additional sampling of similar faunal assemblages originating

464   from other edifices within Lucky Strike would be the next step in testing the consistencies of
465   the differences in faunal assemblages at this vent field.

466

482

483

484   References

485   Bates A. E., Tunnicliffe V., Lee R. W. (2005). Role of thermal conditions in habitat selection
486   by hydrothermal vent gastropods. *Marine Ecology-Progress Series,* **305**, 1-15.

487   Charlou J.L., Dental J.P., Douville E., Jean-Baptiste P., Radford-Knoery J., Fouquet Y.,
488   Dapoigny A., Stievenard M., (2000). Compared geochemical signatures and the evolution of
489   Menez Gwen (37° 50' N) and Lucky Strike (37°17' N) hydrothermal fluids, south of the
490   Azores Triple Junction on the Mid-Atlantic Ridge. *Chemical Geology*, **171**, 49-75

491
492   Chevaldonné P., Desbruyères D., Lehaitre M. (1991). Time-series of temperature from 3
493   deep-sea hydrothermal vent sites. *Deep-Sea Research Part a-Oceanographic Research*
494   *Papers,* **38**, 1417-1430.

495

496   Colaço A., Dehairs F., Desbruyères D. (2002). Nutritional relations of deep-sea hydrothermal
497   fields at the Mid-Atlantic Ridge: a stable isotope approach. *Deep-Sea Research Part I-*
498   *Oceanographic Research Papers,* **49**, 395-412.

499   Comtet T., Desbruyères D. (1998). Population structure and recruitment in mytilids bivalves
500   from the Lucky Strike and Menez Gwen hydrothermal vent fields (37°17'N and 37°50'N on

the Mid-Atlantic Ridge). *Marine Ecology Progress Series,* **163**, 165-177

Cuvelier D., Sarrazin J., Colaço A., Copley J., Desbruyères D., Glover A.G., Tyler P., Serrão Santos R. (2009). Distribution and spatial variation of Atlantic hydrothermal faunal assemblages revealed by high-resolution video image analysis. *Deep Sea Research I- Oceanographic Research Papers,* **56**, 2026–2040.

De Busserolles F., Sarrazin J., Gauthier O., Gélinas Y., Fabri M.C., Sarradin P.M., Desbruyères D. (2009). Are spatial variations in the diets of hydrothermal fauna linked to local environmental conditions? *Deep Sea Research II- Topical Studies in Oceanography,* **56**, 1649-1664.

Desbruyères D., Almeida A., Biscoito M., Comtet T., Khripounoff A., Le Bris N., Sarradin P. M., Segonzac M. (2000). A review of the distribution of hydrothermal vent communities along the northern Mid-Atlantic Ridge: dispersal vs. environmental controls. *Hydrobiologia,* **440**, 201-216.

Desbruyères D., Biscoito M., Caprais J. C., Colaço A., Comtet T., Crassous P., Fouquet Y., Khripounoff A., Le Bris N., Olu K., Riso R., Sarradin P. M., Segonzac M., Vangriesheim A. (2001). Variations in deep-sea hydrothermal vent communities on the Mid-Atlantic Ridge near the Azores plateau. *Deep-Sea Research Part I-Oceanographic Research Papers,* **48**, 1325-1346.

Desbruyères D., Segonzac M., Bright M. (Eds) (2006). *Handbook of deep-sea hydrothermal vent fauna.* Second completely revised edition. Denisia, 18. Biologiezentrum der Oberösterreichischen Landesmuseen. Linz, Austria: 544 pp.

Dreyer J. C., Knick K. E., Flickinger W. B., Van Dover C. L. (2005). Development of macrofaunal community structure in mussel beds on the northern East Pacific Rise. *Marine Ecology Progress Series,* **302**, 121-134.

Fisher C. R., Childress J. J., Arp A. J., Brooks J. M., Distel D., Favuzzi J. A., Felbeck H., Hessler R., Johnson K. S., Kennicutt M. C., Macko S. A., Newton A., Powell M. A., Somero G. N., Soto T. (1988). Microhabitat variation in the hydrothermal vent mussel, *Bathymodiolus thermophilus*, at the Rose Garden vent on the Galapagos Rift. *Deep-Sea Research Part a- Oceanographic Research Papers,* **35**, 1769-1791.

Fisher C. R., (1990). Chemoautotrophic and methanotrophic symbioses in marine invertebrates. *Reviews in Aquatic Science,* **2**, 399-436.

Fouquet Y., Eissen J. P., Ondreas H., Barriga F., Batiza R., Danyushevsky L. (1998). Extensive volcaniclastic deposits at the Mid-Atlantic Ridge axis: results of deep-water basaltic explosive volcanic activity? *Terra Nova,* **10**, 280-286.

Gauthier O., Sarrazin J., Desbruyères D. (2010). Measure and mis-measure of species diversity in deep-sea chemosynthetic communities. *Marine Ecology Progress Series,* **402**, 285-302.

Gebruk A. V., Southward E. C., Kennedy H., Southward A. J. (2000). Food sources, behaviour, and distribution of hydrothermal vent shrimps at the Mid-Atlantic Ridge. *Journal of the Marine Biological Association of the United Kingdom,* **80**, 485-499.

544   Govenar B., Le Bris N., Gollner S., Glanville J., Aperghis A. B., Hourdez S., Fisher C. R.
545   (2005). Epifaunal community structure associated with Riftia pachyptila aggregations in
546   chemically different hydrothermal vent habitats. *Marine Ecology-Progress Series,* **305**, 67-77

547   Henry M. S., Childress J. J., Figueroa D. (2008). Metabolic rates and thermal tolerances of
548   chemoautotrophic symbioses from Lau Basin hydrothermal vents and their implications for
549   species distributions. *Deep-Sea Research Part I-Oceanographic Research Papers,* **55**, 679-
550   695

551   Jannasch H.W. (1985). The chemosynthetic support of life and the microbial diversity at
552   deep-sea hydrothermal vents. *Proceedings of the Royal Society of London, Series B,*
553   *Biological sciences,* **225**, 277-297

554   Johnson K. S., Childress J. J., Beehler C. L. (1988a). Short-term temperature variability in the
555   Rose Garden hydrothermal vent field - an unstable deep-sea environment. *Deep-Sea Research*
556   *Part a-Oceanographic Research Papers,* **35**, 1711-1721

557   Johnson K. S., Childress J. J., Hessler R. R., Sakamoto-Arnold C. M., Beehler C. L. (1988b).
558   Chemical and biological interactions in the Rose Garden hydrothermal vent field, Galapagos
559   Spreading Center. *Deep-Sea Research Part a-Oceanographic Research Papers,* **35**, 1723-
560   1744.

561   Johnson K. S., Childress J. J., Beehler C. L., Sakamoto C. M. (1994). Biogeochemistry of
562   hydrothermal vent mussel communities - the deep-sea analogue to the intertidal zone. *Deep-*
563   *Sea Research Part I-Oceanographic Research Papers,* **41**, 993-1011.

564   Langmuir C., Humphris S., Fornari D., Van Dover C., Von Damm K., Tivey M. K., Colodner
565   D., Charlou J. L., Desonie D., Wilson C., Fouquet Y., Klinkhammer G., Bougault H. (1997).
566   Hydrothermal vents near a mantle hot spot: the Lucky Strike vent field at 37 degrees N on the
567   Mid-Atlantic Ridge. *Earth and Planetary Science Letters,* **148**, 69-91.

568   Le Bris N., Govenar B., Le Gall C., Fisher C.R. (2006). Variability of physico-chemical
569   conditions in 9850VN EPR diffuse flow vent habitats. *Marine Chemistry,* **98**, 167–182
570
571   Legendre P., Gallagher E.G. (2001). Ecologically meaningful transformations for ordination
572   of species data. *Oecologia,* **129**, 271–280
573
574   Luther G. W., Rozan T. F., Taillefert M., Nuzzio D. B., Di Meo C., Shank T. M., Lutz R. A.,
575   Cary S. C. (2001). Chemical speciation drives hydrothermal vent ecology. *Nature,* **410**, 813-
576   816.

577   Lutz R. A., Shank T. M., Luther G. W., Vetriani C., Tolstoy M., Nuzzio D. B., Moore T. S.,
578   Waldhauser F., Crespo-Medina M., Chatziefthimiou A. D., Annis E. R., Reed A. J. (2008).
579   Interrelationships between vent fluid chemistry, temperature, seismic activity, and biological
580   community structure at a mussel-dominated, deep-sea hydrothermal vent along the East
581   Pacific Rise. *Journal of Shellfish Research,* **27**, 177-190.

582   Martins I., Colaco A., Santos R. S., Lesongeur F., Godfroy A., Sarradin P. M., Cosson R. P.
583   (2009). Relationship between the occurrence of filamentous bacteria on Bathymodiolus
584   azoricus shell and the physiological and toxicological status of the vent mussel. *Journal of*
585   *Experimental Marine Biology and Ecology,* **376**, 1-6.

Matabos M., Le Bris N., Pendlebury S., Thiébaut E. (2008). Role of physico-chemical environment on gastropod assemblages at hydrothermal vents on the East Pacific Rise (13°N/EPR). *Journal of the Marine Biological Association of the United Kingdom,* **88**, 995-1008

Menge B.A., Sutherland J.P. (1976). Species diversity gradients: synthesis of the role of predation, competition and temporal heterogeneity. *The American Naturalist,* **110**, 351-369

Mills S. W., Mullineaux L. S., Tyler P. A. (2007). Habitat associations in gastropod species at East Pacific Rise hydrothermal vents (9 degrees 50 ' N). *Biological Bulletin*, **212**, 185-194.

Oksanen J., Kindt R., Legendre P., O'Hara B., Simpson G.L., Solymos P., Stevens M.H.M., Wagner H. (2008). vegan: Community Ecology Package. R package version 1.15-0. http://cran.r-project.org/S, http://vegan.r-forge.r-project.org/.

Ondréas H., Cannat M., Fouquet Y., Normand A., Sarradin P. M., Sarrazin J. (2009). Recent volcanic events and the distribution of hydrothermal venting at the Lucky Strike hydrothermal field, Mid-Atlantic Ridge. *Geochemistry Geophysics Geosystems,* **10** (2).

Podowski E.L., Moore T.S., Zelnio K.A., Luther III G.W., Fisher C.R. (2009). Distribution of diffuse flow megafauna in two sites on the Eastern lau Spreading Center, Tonga. *Deep Sea Research I-Oceanographic Research Papers,* **56**, 2041-2056

Sarradin P. M., Caprais J. C., Briand P., Gaill F., Shillito B., Desbruyères D. (1998). Chemical and thermal description of the environment of the Genesis hydrothermal vent community (13°N, EPR). *Cahiers de Biologie Marine,* **39**, 159–167.

Sarradin P. M., Caprais J. C., Riso R., Kerouel R., Aminot A. (1999). Chemical environment of the hydrothermal mussel communities in the Lucky Strike and Menez Gwen vent fields, Mid Atlantic Ridge. *Cahiers de Biologie Marine,* **40**, 93-104.

Sarradin P.M., Waeles M., Bernagout S., Le Gall C., Sarrazin J., Riso R. (2009). Speciation of dissolved copper within an active hydrothermal edifice on the Lucky Strike vent field (MAR, 37°N). *Science of the Total Environment,* **407**, 869-878

Sarrazin J., Robigou V., Juniper S. K., Delaney J. R. (1997). Biological and geological dynamics over four years on a high-temperature sulfide structure at the Juan de Fuca Ridge Hydrothermal Observatory. *Marine Ecology-Progress Series,* **153**, 5-24.

Sarrazin, J., Juniper, S.K. (1999). Biological Characteristics of a Hydrothermal Edifice Mosaic Community. *Marine Ecology Progress Series,* **185**, 1-19

Sarrazin J., Juniper S. K., Massoth G., Legendre P. (1999). Physical and Chemical Factors Influencing Species Distributions on Hydrothermal Sulfide Edifices of the Juan De Fuca Ridge, Northeast Pacific. *Marine Ecology Progress Series,* **190**, 89-112.

Sarrazin J., Walter C., Sarradin P.M., Brind'Amour A., Desbruyères D., Briand P., Fabri M.C., Van Gaever S., Vanreusel A., Bachraty C., Thiébaut E. (2006). Community structure and temperature dynamics within a mussel community on the southern East Pacific Rise. *Cahiers de Biologie Marine,* **47**,483–490

630 Shillito B., Le Bris N., Hourdez S., Ravaux J., Cottin D., Caprais J. C., Jollivet D., Gaill F.
631 (2006). Temperature resistance studies on the deep-sea vent shrimp Mirocatis fortunata.
632 *Journal of Experimental Biology,* **209**, 945-955.

633 Tsurumi M., Tunnicliffe, V. (2003). Tubeworm-associated communities at hydrothermal
634 vents on the Juan De Fuca Ridge, Northeast Pacific. *Deep-Sea Research Part I-*
635 *Oceanographic Research Papers,* **50**, 611-629.

636 Urcuyo I.A., Massoth G.J., Julian, D., Fisher, C.R. (2003). Habitat, growth andphysiological
637 ecology of a basaltic community of Ridgeia piscesae from the Juan de Fuca Ridge. *Deep-Sea*
638 *Research Part I-Oceanographic Research Papers,* **50**, 763-780

639 Van Dover C.L., Trask J.L. (2000). Diversity at Deep-Sea Hydrothermal Vent and Intertidal
640 Mussel Beds. *Marine Ecology Progress Series,* **195**, 169-178.
641
642 Vuillemin R., Le Roux D., Dorval P., Bucas K., Sudreau J.P., Hamon M., Le Gall C.,
643 Sarradin P. M. (2009). CHEMINI: a new in situ CHEmical MINIaturized analyzer. *Deep-Sea*
644 *Research Part I-Oceanographic Research Papers,* **56**, 1319-1399
645
646
647
648
649
650
651
652
653
654
655
656
657
658
659
660
661
662
663
664
665
666
667
668
669
670
671
672

Tables

676 Table 1: Species densities (ind/m²) and total taxonomic richness in the different faunal
677 assemblages sampled. The undetermined species were also considered in the taxonomic
678 richness and rarefaction calculations as these were definitely different from the other
679 determined species. Highly mobile *Segonzacia mesatlantica* (Bythograeidae, Decapoda) crabs
680 were left out of the table. As=Assemblage

681

Group	Species	Density (ind/m²)				
		As_1	As_2a	As_2b	As_3	As_4a
Mollusca						
Bivalvia						
Mytilidae	*Bathymodiolus azoricus*	952	**5027**	569	0	3260
Gastropoda						
Lepetodrilidae	*Lepetodrilus atlanticus*	0	**340**	0	0	104
	Pseudorimula midatlantica	0	0	0	0	21
Skeneidae	*Protolira valvatoides*	0	**1155**	0	0	1121
Orbitestellidae	*Lurifax vitreus*	0	**68**	0	0	0
Phenacolepadidae	*Shinkailepas briandi* (empty)**	0	0	44	0	21
Polychaeta						
Polynoidae	*Branchipolynoe seepensis*	385	**544**	350	0	332
	Branchinotogluma mesatlantica	**18**	0	0	0	0
Ampharetidae	*Amathys lutzi*	**330**	68	219	0	249
	Polychaeta indet.	37	0	**88**	0	21
	Polynoidae indet.	0	0	0	**27**	21
Arthropoda						
Amphipoda						
Eusiridae	*Luckia striki*	0	136	**832**	27	21
	Amphipoda indet.	0	**68**	0	0	0
Decapoda						
Alvinocarididae	*Mirocaris fortunata*	604	0	3065	**3406**	62
Pycnogonida						
Ammotheidae	*Sericosura heteroscela*	0	0	0	0	**123**
Surface sampled cm²		546.12	147.21	228.41	369.98	481.66
Taxonomic richness		6	8	6	3	**11**
Rarefaction Es(100)		5.74	7.75	5.98	2.56	**8.19**

682 **Not considered in statistical analyses or diversity calculations
683
684
685
686
687
688
689
690
691
692
693
694

695

696

697 Table 2: Mean values of T°C, ∑S and CH$_4$ and their standard deviations (stdev) measured or
698 estimated on the different faunal assemblages. T°C and ∑S were measured *in situ*, n=number
699 of samples, which is absent for CH$_4$ as this factor was calculated from the *in situ* T°C values,
700 using a T°C vs. CH$_4$ regression curve. Maximum values are highlighted in grey.

701

702

	T°C		∑S total µM		CH$_4$ total µM (estimated)
	n	**Mean ± stdev**	**n**	**Mean ± stdev**	**Mean ± stdev**
Assemblage 1	120	5.12 ± 0.39	7	1.72 ± 0.73	5.59 ± 0.75
Assemblage 2a	129	5.37 ± 0.13	6	1.40 ± 0.37	6.20 ± 0.17
Assemblage 2b	116	4.71 ± 0.15	7	0.81 ± 0.29	4.76 ± 0.28
Assemblage 3	128	6.79 ± 0.88	8	9.00 ± 11.81	8.73 ± 3.10
Assemblage 4a	117	4.81 ± 0.07	6	4.47 ± 0.83	4.96 ± 0.08
Assemblage 4b	115	5.01 ± 0.10	4	3.64 ± 0.87	5.61 ± 0.11

703
704
705
706
707
709
710

711

712

713

714

715

716

717

718

719

720

721

722

723

724

725

726

727

728

729

730

731

732

733

734

735

736

737

738

Figures
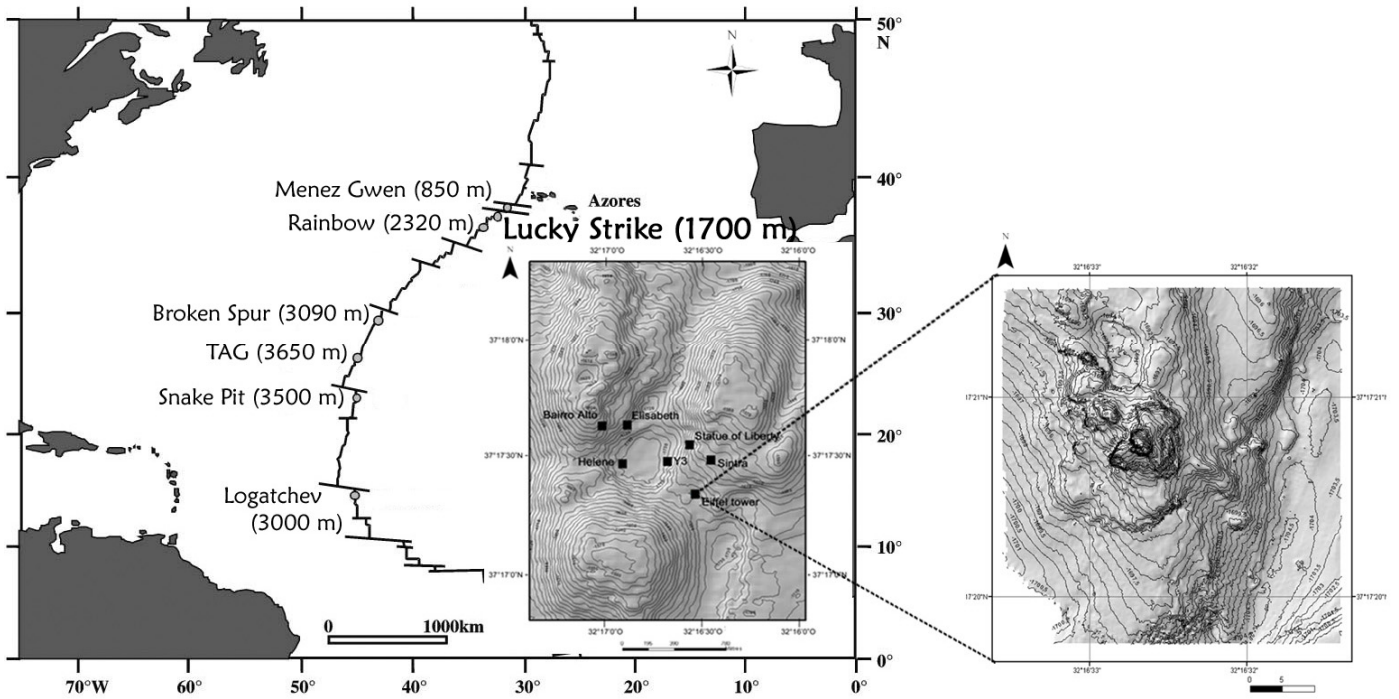
761
762 Fig. 1: Major known vent fields and their respective depths are shown along the Mid-Atlantic
763 Ridge. The inset shows the Lucky Strike vent field with several of its most well-defined
764 edifices. The 11m high Eiffel tower is one of them, situated in the south-eastern sector of the
765 vent field.
766
767
768
769
770
771
772
773
774
775
776
777
778
779
780
781
782
783
784
785
786
787
788
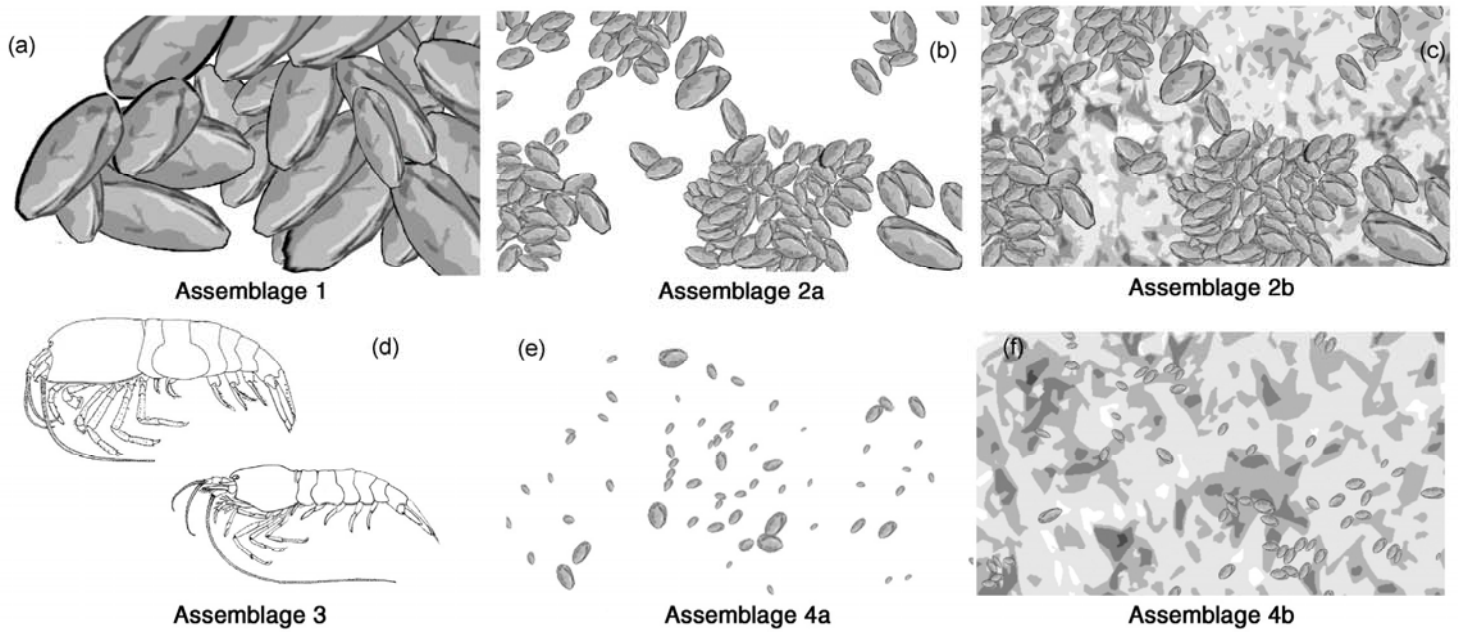
Fig. 2: Assemblage identification based on imagery as described by Cuvelier et al. (2009), varying in visibly dominant species (mussels and shrimp), in mussel size and in density of mussel coverage. Each assemblage is represented by a sketch (a) Assemblage 1: dense *Bathymodiolus azoricus* mussel beds of larger-sized mussels (~6 cm), (b) Assemblage 2a: mussel clumps of smaller sized mussels (2-5 cm) with bare substrata in between, (c) Assemblage 2b: Assemblage 2a but with a microbial cover (d) Assemblage 3: alvinocaridid shrimp colonising bare surface (mostly *Mirocaris fortunata*, other shrimp species can be recognised on imagery), (e) Assemblage 4a: scattered small mussels (~1cm) with prevailing bare surface and (f) Assemblage 4b: Assemblage 4a but with a microbial cover.
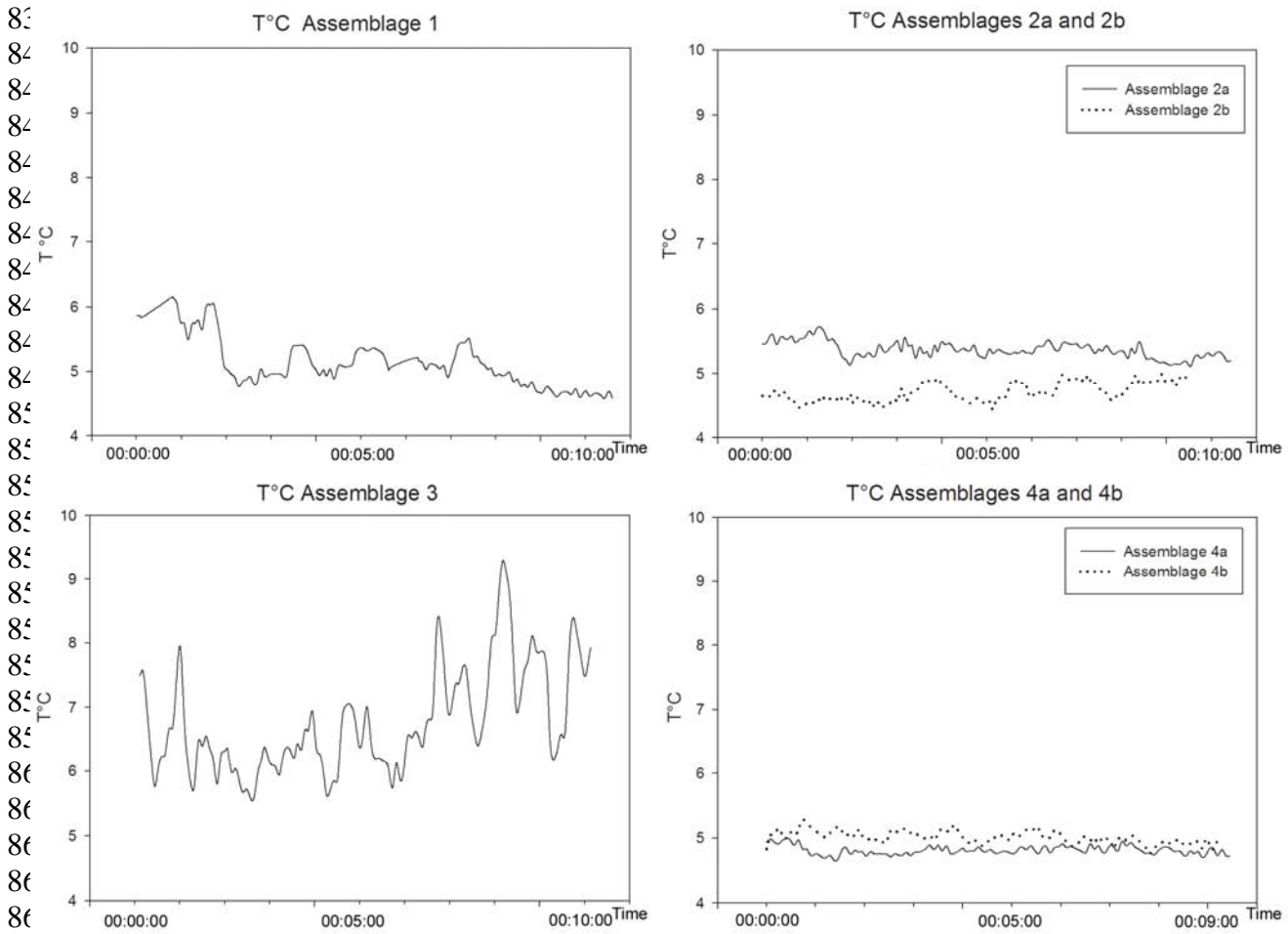
Fig. 3. Temperature fluctuations over a 10 minute time period on the different assemblages sampled.
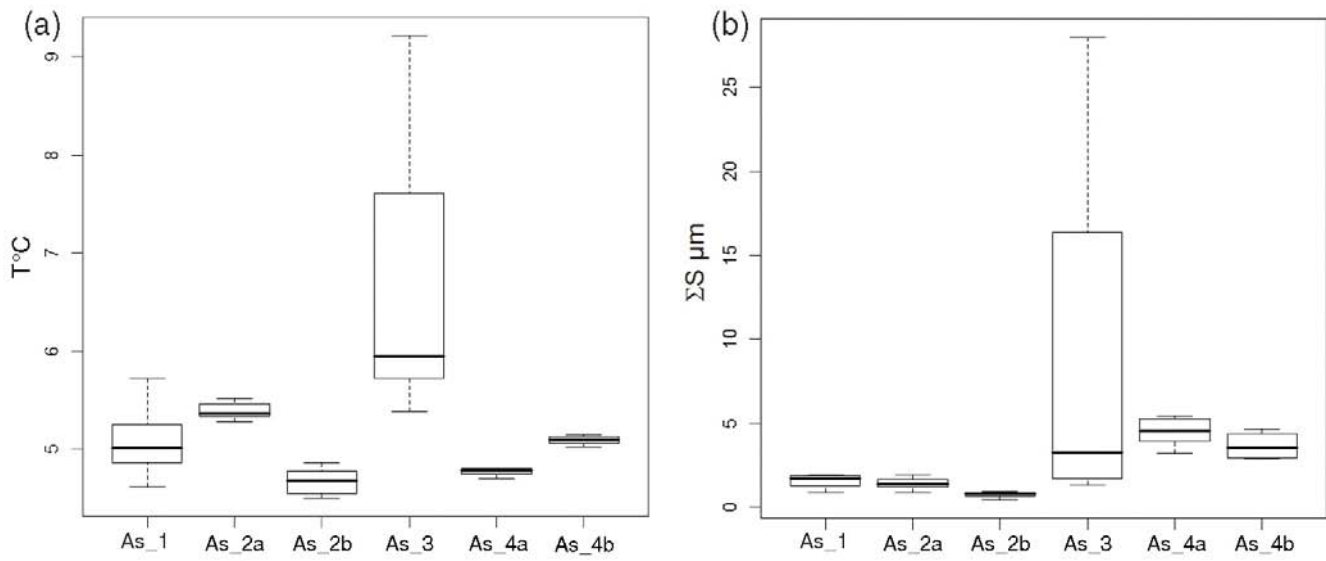
Fig. 4: Boxplots of environmental variables per assemblages. (a) Temperature and (b) ΣS were measured *in situ*. Black horizontal lines within the boxes represent the median.
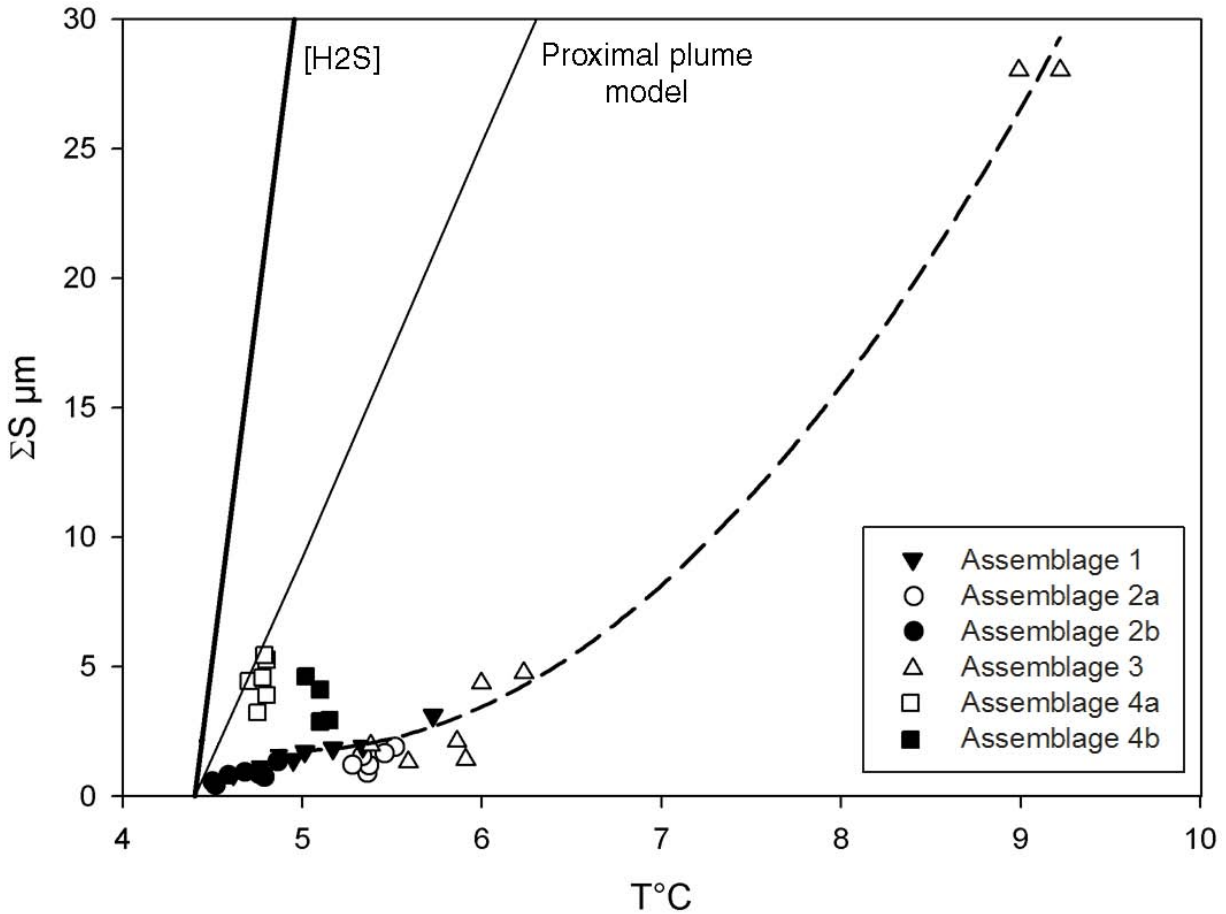
Fig. 5: Total sulfide concentration versus temperature on the different assemblages of the Eiffel Tower edifice. The curve between the assemblages is the best fitting polynomial curve ($R^2=0.95$) and can be considered as a non-linear dilution curve. [H_2S] is the theoretic sulfide value, based on the end-member fluid concentrations at Eiffel Tower (Charlou et al., 2000). The "proximal plume model" represents the T°C vs. ΣS values based on the measurements made on uncolonised areas, in the vicinity of a black smoker (Sarradin et al., in prep.). See Fig. 2 for assemblage identification.
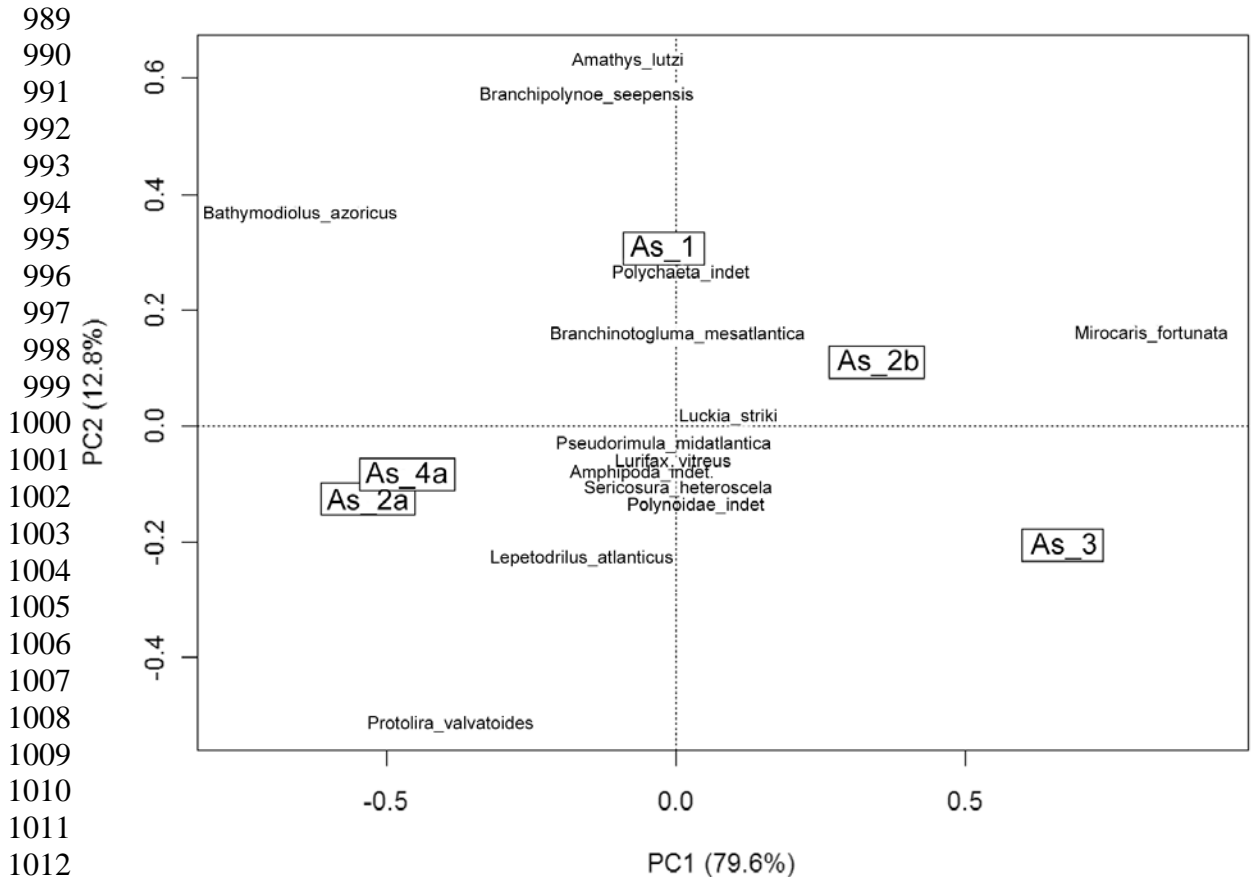
Fig. 6: Principle Components Analysis (PCA) based on the Hellinger transformed species abundance data. A total variation of 92.4% is explained by the PCA plot, where the first axis accounts for 79.6% and the second for 12.8%. Ass=Assemblage.
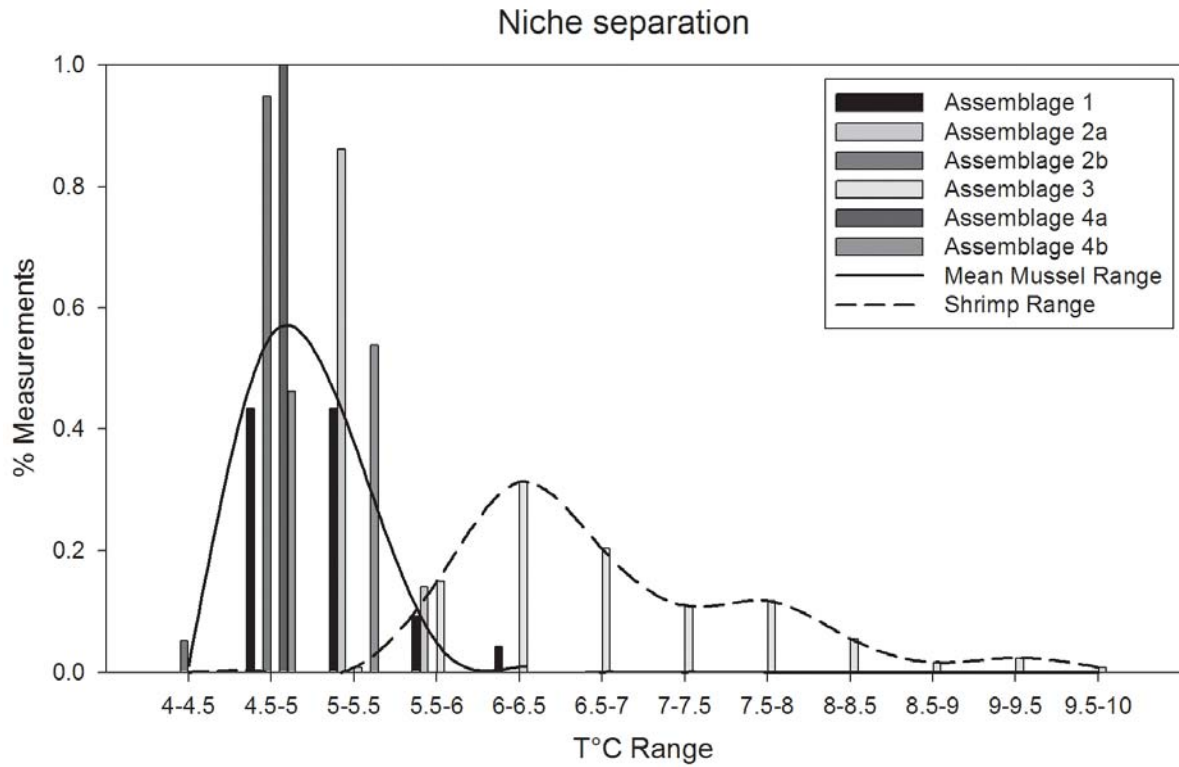
Fig. 7. Histogram featuring the percentage of T°C measurements in 0.5°C intervals for each assemblage. Two temperature-niches are revealed, one for the mussel-based assemblages (mean frequency) of the mussel-based assemblages measurements) and the other for the shrimp assemblage.